Journal of the Maharaja Sayajirao University of Baroda
ISSN: 0025-0422

Sol-gel autombustion lab-scale production and materialistic investigation of Ni(0.8-x)Cu(x)Zn(0.2)Fe2O4 nanoferrites

Vidyadhar Awati* Department of Physics, Chandmal Tarachand Bora College, Shirur, Dist: Pune, (MS), 412210 India
Sopan Rathod P.G.Department of Physics, Abasaheb Garware College, Pune, Pin- 411004 India
Popat Virkar Department of Chemistry, Chandmal Tarachand Bora College, Shirur, Dist : Pune, (MS), 412210 India
Kiran Badave Department of Chemistry, Chandmal Tarachand Bora College, Shirur, Dist : Pune, (MS), 412210 India
Dattatray Bobabde Department of Physics, Chandmal Tarachand Bora College, Shirur, Dist: Pune, (MS), 412210 India

Abstract:
Copper doped NiCuZn ferrites were synthesiesed by autocombustion method for studying structural and magnetic inheritance. The nanopowders of Ni(0.8-x)Cu(x)Zn(0.2)Fe2O4 ferrites for x as a copper scaling 0.0 to 0.8 with advancement of 0.20 are produced. Formation of spinel structure with single-phase proved by x-ray diffraction impressions. The lattice specifications alongwith grain size calculated from X-ray data. The synthesiesed nanoferrites particle size ranges from 6 μm to 61 μm. The scanning electron microscope is used to study morphology. LCR meter determines the dielectric constant and its variation with frequency and temperature. Prepared analytes obey inter-facial polarization as predicted by Maxwell -Wagner. Variation in saturation-magnetization (Ms) is observed 70.821 emu/g to 64.982 emu/g. These synthesiesed nanoferrites has applications in primitive materials and electronic gadgets
Key words: ferrites; Combustion synthesis; dielectric constant; magnetization in magnetic materials
PACS : 75.50.Gg , 81.20.Ka , 78.20.Ci , 75.60.E

Introduction

Nickel-Copper-Zinc ferrites are spinel in nature. They are soft type magnetic materials, having applications in sensors for measurement of temperature and humidity, multi-layer chip-inductor (MLCIs) and multi-layer LC-filters etc. Due to unique magnetic properties soft magnetic materials having nano-meter size are widely accepted. The inheritance of such fabricated nanopowders are very dissimilar from their bulge analogue. [1] With high saturation magnetization and high permeability the magnetic nanomaterials show no remnant magnetization and coercivity which indicates its supermagnetic nature. Due to unique properties of nanosized soft NiCuZn ferrites, researchers focused their interest on synthesizing them over their bulk form. Copper doped ferrites are fascinating because of wide applications in electro-magnetic materials. During synthesis copper doped ferrites undergoes structural phase transition along with changes in crystal symmetry [2, 3]. NiCuZn nanoferrites can be synthesiesed by various methods. The variation in physical and magnetic properties of nanoferrites alters with particle size. The particle size depends upon the route of synthesis, type of doping metals and concentration. [4, 5].

These observations from earlier study leads to look into function of Copper on dimensional, electro-magnetic inheritance in NiCuZn fabricated nano-ferrites. Special properties like high electric resistivity along with soft magnetic nature at elevated frequencies creates new gateway for improving devices like mounting of electrical components and multilayer chip-inductors (MLCI). These devices have wide applications in telecommunication field. The efficacy SMD, MLCI depend on structural, electro-magnetic inheritance of the fabricated nanomaterials. Advanced investigative study is must for complete conversance of such type of nano-solids.

Materials and Methods

Lab scale manufacturing of Nanoferrites:

$Ni_{(0.8-x)}Cu_{(x)}Zn_{(0.2)}Fe_2O_4$ (x = 0.0, 0.2, 0.4, 0.6, and 0.8) nanopowder fabricated through sol-gel route. Metal nitrates i.e. $Cu(NO_3)_2$, $Zn(NO_3)_2$, $Ni(NO_3)_2$, and $Fe2(NO_3)_2$ of analytical reagent standard are utilized for synthesis. These nitrates solubilized in ultrapure water and heated to 80o C upto 20 minutes. Citric acid added in metal nitrate solution and pH of solution is kept neutral by adding liquid ammonia and then heated continuously with stirring at temperature 100o C. On complete dehydration it converts into the viscous gel. After a while formed semi-solid mass gets combusted and incinerate rapidly. This completes auto-combustion process giving brown colored ashes. Synthesized ferrite powders sintered at 1000o C for 3 to 4 hours. Now Nanopowder is pressed to get pellets of 11 mm diameter using hydraulic press by exerting pressure of 120 kg / cm2 for few minutes. Pellets were heated at 1000o C for 3 to 4 hours.

Characterization

Model Bruker D8 X- ray diffractometers is utilized to get X- ray diffraction (XRD) pattern. XRD data utilized to estimate lattice parameter, crystallite (grain) size and porosity. To elucidate dimensional study and to determine grain size Scanning Electron Microscope, (SEM) is used. LCR meter (HP 4284 A) with 100 Hz to 1 MHz is used to measure dielectric constant, loss factor (tan δ) at ambient environment. Magnetic inheritance of fabricated nanopowder in the field of 10 kOe is studied using Vibrating Sample Magnetometer (VSM) in ambient environment.

Results and Discussions:

Structural Analysis:

Fig. 1 represents XRD peaks of $Ni_{(0.8-x)}Cu_{(x)}Zn_{(0.2)}Fe_2O_4$ ferrites where doping element. Copper quantity (x) with x = 0.0, 0.2, 0.4, 0.6,0.8 made using solgel route. The diffraction data confirms spinel structure with ferrite state for prepared nanopowders. XRD patterns reveals that relative intensity along with vertex point of each diffracted signal correlates with standard powder diffraction data [6]. The absence of impurity peak and presence of broad XRD peaks indicates the formation of highly pure nanoferrite powder. The Scherrer formula [7] is used to estimate the mean grainsize for every set from (311) plane of the XRD peak. Table 1 summarizes the values calculated from XRD data for crystalline size and lattice parameter. The lattice parameter enhanced alongwith raising concentration of cupric (Cu2+) ions since ionic radius of cupric (Cu2+) ions (0.730 Å) is more as compared to ionic radius of Ni ions (0.690Å) [8]. This confirms formation of cubic spinel structural ferrites [9-12]. Sintered powder XRD patterns do not show presence of any unidentified peaks indicating that there is no diffusion or any chemical reaction took place [13].

The equation (1) determines sintered density (d_s):

$$\boldsymbol{ds = m} \div \pi r^2 h \quad \text{-------- (1)}$$

Here, d_s – sintered density, m - mass, r - radius, h - width of sample.

Table 1 shows the variation in sintered density from 4.191 g/cm^3 to 4.706 g/cm^3 as a result of ionic variation among Ni and Cu [14-17] and may be owing to larger density of copper (8.96 g / cm^3) over nickel (8.90 g / cm^3). Equation (2) given by Smit and Wijin is utilized to determine x-ray density (d_X) [18].

$$\boldsymbol{dx = 8M} \div N_a a^3 \quad \text{------ (2)}$$

Here, d_x - X-rays density, M – sample molecular weight, N_a - Avogadro's number, 'a' - lattice constant.

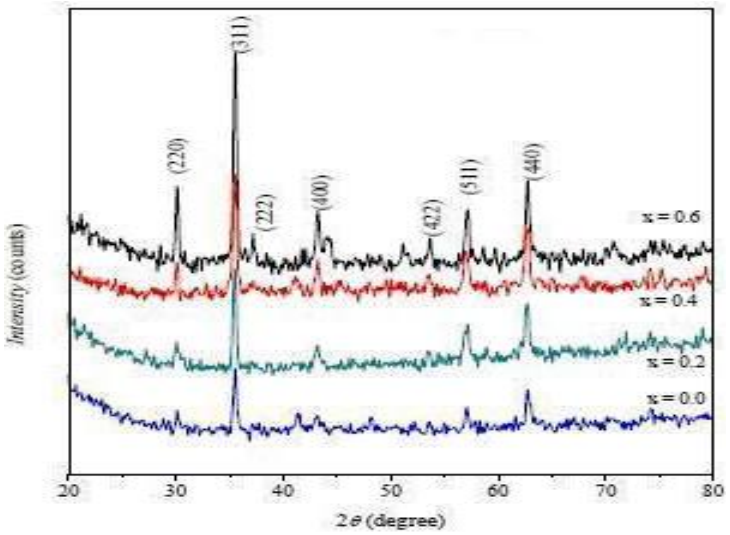

Figure 1. X-Ray Diffraction Data of $Ni_{(0.8-x)}Cu_{(x)}Zn_{(0.2)}Fe_2O_4$ ferrites.

Variation in X-ray density is form 5.401 g / cm^3 to 5.390 g / cm^3. The inverse relation between lattice constant and x-ray density is seen from Table 1, as Cu concentration increases lattice constant (a) enhances while relative x-ray density (dx) falls down.

The equation (3) is utilized to determine percentage porosity (P) of fabricated analytes.

$$\boldsymbol{P = \left(1 - \frac{ds}{dx}\right) * 100} \text{ --------- (3)}$$

Composition (X)	Lattice Parameter 'a' (Å)	Grain-size (μm)	Sintered-Density (d_s)	X-ray Density (d_x)	% Porosity (P)
0.0	8.340	6.09	4.191	5.397	2.24
0.2	8.360	13.27	4.319	5.396	1.99
0.4	8.364	28.82	4.560	5.395	1.55
0.6	8.374	52.12	4.655	5.393	1.40
0.8	8.391	61.27	4.706	5.392	1.12

Table 1: Lattice Parameter (a), Grain size, Sintered density (d_s), X-ray density (d_x), Porosity (P) of $Ni(0.8-x)Cu(x)Zn_{(0.2)}Fe_2O_4$ nanoferrites.

Table 1 indicates percentage porosity decreases from 2.24 % to 1.12 %. With rise in Cu concentration it is observed that sintering density rises and X-ray density decreases and it leads to decrease in porosity. It also justified in aotherway as creation of more oxygen vacancies after doping Cu decreases the porosity as less number of cations are generated. Also existence of pores in sample confirms the high value of x-ray density with corresponding sintered density.

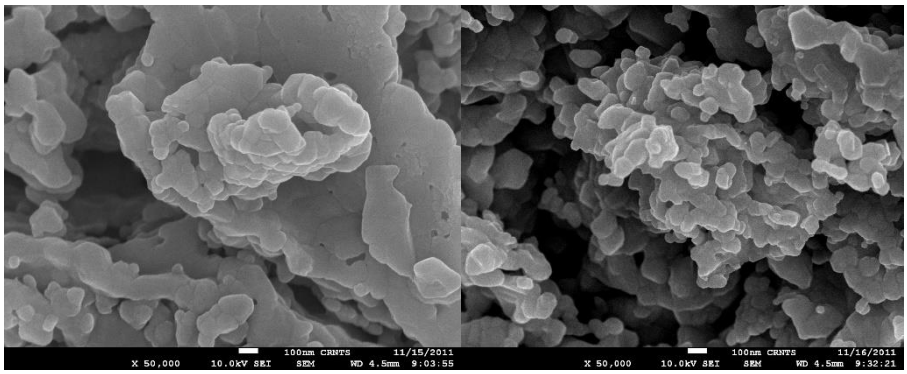

$Ni_{0.8}Cu_{0.0}Zn_{0.2}Fe_2O_4$ $Ni_{0.6}Cu_{0.2}Zn_{0.2}Fe_2O_4$

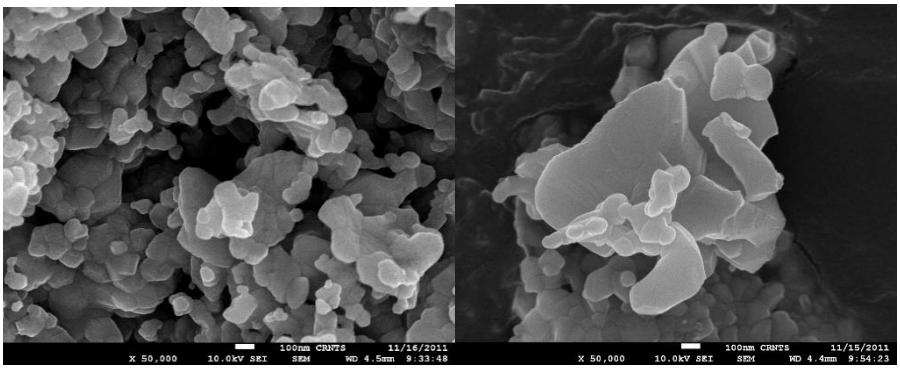

$Ni_{0.4}Cu_{0.4}Zn_{0.2}Fe_2O_4$ $Ni_{0.2}Cu_{0.6}Zn_{0.2}Fe_2O_4$

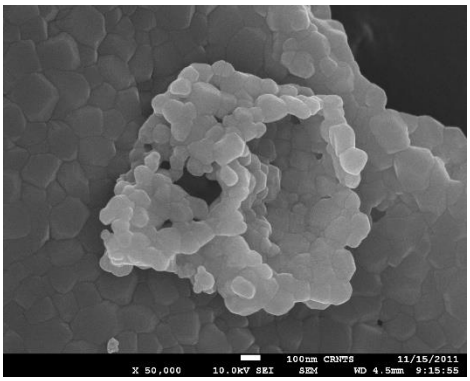

$Ni_{0.0}Cu_{0.8}Zn_{0.2}Fe_2O_4$

Figure 2. Typical SEM micrographs of $Ni_{(0.8-x)}Cu_{(x)}Zn_{(0.2)}Fe_2O4$ ferrites for X = 0.0 to 0.8.

Fig 2. Shows the images of $Ni_{(0.8-x)}Cu_{(x)}Zn_{(0.2)}Fe_2O_4$ ferrites using scanning electron microscope. This helps to study surface morphology. The micrographs reveals that as increase in Cu substitution enhances the granule size by 6.09 μm to 61.27 μm which correlates earlier published data. As Cu ions have higher atomic mobility, it rises granule size as noted by Dimri et.al. [19, 20]. Micrographs exhibits ferrite particles are of similar size and agglomeration occurred at some particles.

Dielectric Properties:
The equation (4) is used to calculate dielectric constant

$$\boldsymbol{\varepsilon = Ct} \div \varepsilon_o A \quad \text{---------- (4)}$$

Here, C - pellet capacitance in farad, t - pellet thickness in meters, A - flat surface cross-sectional area, ε_o - constant of permittivity in vacuum.

Frequency dependence of dielectric constant:

Ferrites are combination of multiple structural and microstructural elements. Fig. 3 indicates configurational changes of dielectric-constant with 10.0 kHz frequency. Rise in Cu concentration rises dielectric constant that leads to increment in possibilities of electrons arriving grain boundary simultaneously decreases resistivity. This results into enhancement in polarization and dielectric constant. Fig. 4 indicates fluctuation in dielectric constant (έ) alongwith frequency. At lesser frequencies dielectric constant is more. As frequency boost the dielectric constant declines. Dielectric constant steep downwards upto 1 kHz, then further lowers upto 10 kHz and remains steady farther10 kHz [21]

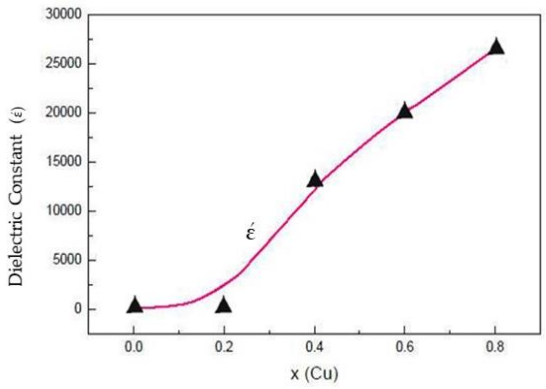

Figure 3. Variation of Dielectric constant with (Cu) at 10 kHz for $Ni_{(0.8-x)}Cu_{(x)}Zn_{(0.2)}Fe_2O_4$ Ferrites.

Maxwell-Wagner group inter-facial polarization is observed in all the samples which is in conformance with Koop's Theory [22]. At low frequencies higher values of dielectric constants are noted. This is correlated with space charge polarization accompanied by nonuniform dielectric structure such as impurity, porosity, grain structure and resistivity of fabricated analytes.

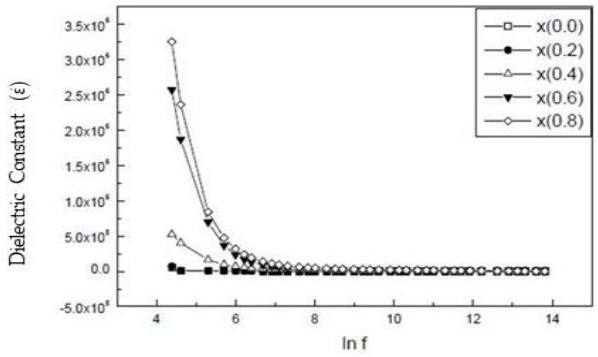

Figure 4. Change in dielectric constant 'ε' with frequency 'lnf' for $Ni_{(0.8x)}Cu_{(x)}Zn_{(0.2)}Fe_2O_4$ ferrites.

Modification of dielectric constant alongwith frequency is studied by many researchers and they concluded that process of dielectric polarization is congruent to conduction [23, 24]. In ferrites electron exchange interaction occurs between ferrous ion to ferric ion ($Fe^{2+} \rightarrow Fe^{3+}$) and Nickel (2+) to Nickel (3+) which causes local electrons displacement towards electric field. This is main cause of polarization in ferrites. Dielectric behaviour 'ε' changes alongwith frequency and accomplishes certain value of frequency. Beyond this frequency exchange of electron does not abide by electric field**.**

Frequency (f) reliance of dielectric loss tangent (tan δ) :

Change in dielectric loss tangent 'tan δ' with applied frequency 'log f' for fabricated analytes shown in figure 5. It shows unusual dielectric pattern showing maxima at particular frequency. Such type of behaviour is also reported for Copper-Cadmium,[25] Lithium –Magnesium-Titanium[26], Nickel-Magnesium[27], Magnesium-Zinc[28] ferrites. The peaks are more prominent in $Ni_{(0.8-x)}Cu_{(x)}Zn_{(0.2)}Fe_2O_4$ ferrites for x = 0.0, 0.2, 0.4, 0.6,0.8 than that of earlier reported investigations. Table 1 shows the frequency and tan δ values for each fabricated sample.

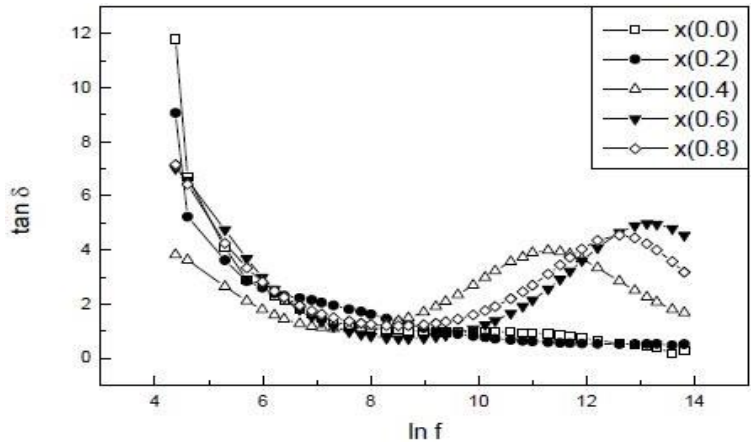

Figure 5. Change in loss factor 'tan δ' with frequency 'ln f' for $Ni_{(0.8-x)}Cu_{(x)}Zn_{(0.2)}Fe_2O_4$ ferrites.

The relaxation relation gives the condition for observing a maximum [29].

$$\boldsymbol{\tau * \omega = 1} \quad \text{---------} \ 5$$

Here τ = relaxation time and $\omega = 2\pi f_{max}$

Magnetic Properties

Figure 6 shows the change of saturation magnetization (M_s) with Copper composition. Saturation magnetization (M_s) declines with cupric (Cu^{2+}) ion concentration. At particular composition i.e. at x = 0.8 it reaches minimum. This is due to cation-distribution alongwith exchange interaction as occupation of cations in A- and B-sites affects magnetic behaviour of ferrites. It

is noted that the saturation magnetization (M_s) reduces by 70.821 emu/g to 64.982 emu/g alongwith rise in copper content. As the value of magnetic moment of copper is lower than that of nickel [30].

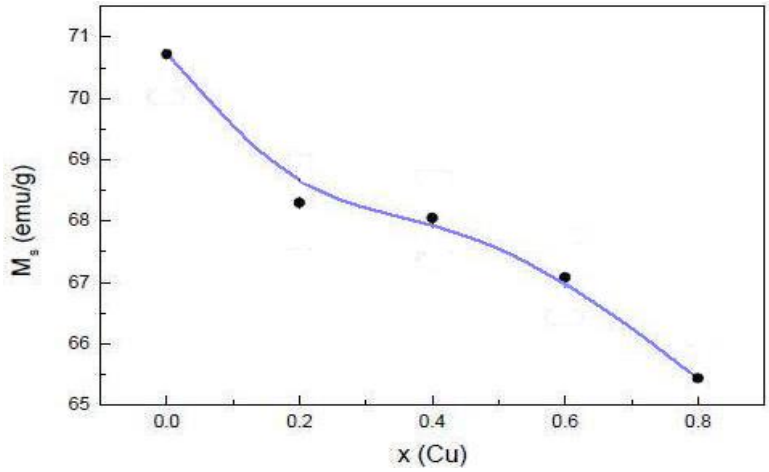

Figure 6. Saturation magnetization as function of x (Cu) for $Ni_{(0.8-x)}Cu_{(x)}Zn_{(0.2)}Fe_2O_4$ ferrites.

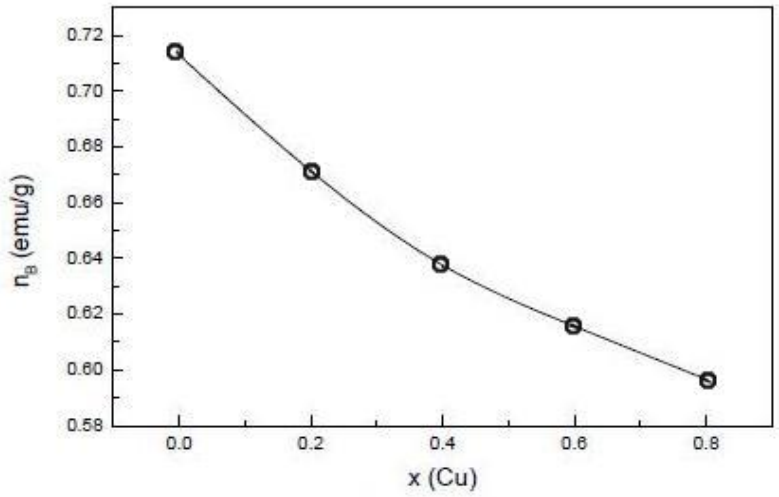

Figure 7. Graph of magnetic moment (Ms) verses concentration of x (Cu) for $Ni_{(0.8-x)}Cu(x)Zn_{(0.2)}Fe_2O_4$ ferrites.

Equation 6 is used to calculate Magnetic moment (n_B):

$$\boldsymbol{nB = Mol.Wt * Ms \div 5585d} \quad \text{---------- 6}$$

Here n_B = magnetic moment, M_s = saturation magnetization and d_s = sintered density

Figure 7 shows a graph of magnetic moment 'n_B' verses composition of Copper for prepared ferrites. At B-site total magnetic moment reduces by replacement of Cuprous ions (Cu^{2+}) at octahedral site rather Nickel (Ni^{2+}) ions. In NiCuZn ferrites the diminishing of A-B interrelationship decreases net magnetization as magnetic moment of cuprous ions is smaller as compared to magnetic moment of Ni^{2+}. The values of magnetic moment from 0.783 emu/g to 0.592 emu/g shows declined trend as reflected in Figure 7.

Conclusions

Nano-crystalline NiCuZn ferrites are formed by autocombustion route. Formation of cubic spinel structure with single phase approved by XRD patterns. Increase in copper concentration results into decline of porosity and x-ray density for prepared analytes while sintered density and lattice constant rises. Particle size of prepared samples varies from 6 µm to 61 µm. With increase in copper concentration the dielectric constant increases as conductivity of copper is better than nickel. Space charge polarization process is the cause of variation in tanδ and ε and decreases with rise in frequency. Decrease in saturation magnetization (Ms) and magnetic moment (nB) is noted. Remarkable modifications were observed in structural and electrical

attributes due to doping of Copper in $Ni_{(0.8-x)}Cu_{(x)}Zn_{(0.2)})Fe_2O_4$ ferrites. Thus $Ni_{(0.8-x)}Cu_{(x)}Zn_{(0.2)})Fe_2O_4$ composition becomes a promising candidate for MLC technological applications.

Acknowledgments:

Researchers acknowledges DST for the availability of instruments under DST-FIST programme at C. T. Bora College, Shirur (DST-FIST File No: SR/FST/COLLEGE/068/2017)

Conflicts of Interest: The authors declare no conflict of interest

References

[1] Kumar, R.; Kamzin, A. S.; Prakash, T. Effect of particle size on structural, magnetic and dielectric properties of manganese substituted nickel ferrite nanoparticles *Journal of Magnetism and Magnetic Materials* **March 2015**, Vol. 378, pp. 389-396 https://doi.org/10.1016/j.jmmm.2014.11.019

[2] Das, P. S.; Singh, G. P. Structural, magnetic and dielectric study of Cu substituted NiZn ferrite Nanorod *Journal of Magnetism and Magnetic Materials* **2016,** Vol. 401, pp.918–924 https://doi.org/10.1016/j.jmmm.2015.10.132

[3] Li, Q∗.; Wang, Y., Chang, C. Study of Cu, Co, Mn and La doped NiZn ferrite nanorods synthesized by the coprecipitation method *Journal of Alloys and Compounds* **2010** ,Vol- 505, pp. 523–526 https://doi.org/10.1016/j.jallcom.2010.06.132

[4] Shaikh, S; Ubaidullah, M; Mane, R. S.; Al-Enizi, A. M. CHAPTER 4 Types, Synthesis methods and applications of ferrites, Spinel Ferrite Nanostructures for Energy Storage Devices, Mane, R. S; Jadhav, V. **June 2020**, pp. 51–82. ISBN 978-0-12-819237-5 Elsevier Inc. doi:10.1016/b978-0-12-819237-5.00004-3

[5] Kanamadi, C.M. Impact of copper on structural and magnetic properties of NiZn ferrites for multi-layer chip inductor Materials Today: Proceedings, International Conference on Multifunctional and Hybrid Materials for Energy and Environment MHMEE-**2020**, Yashavantrao Chavan Institute of Science, Satara, India, 29-31 January, **2020** https://doi.org/10.1016/j.matpr.2020.06.479

[6] Smith, D. K; McCarthy G. J; Bayliss, P; and Fitzpatrick, J; **1986**, PDF Mineral File Workbook: Use of the X-ray Powder Diffraction File of Minerals JCPDS International Centre for Diffraction Data. Swarthmore, PA, U.S.A.

[7] D, Cullity Elements of X-ray diffraction Publisher - Addison-Wesley Publish. Co.; England 1967; pp. 42

[8] Thakur, A. Mathur, P. Singh, M. Controlling the properties of Mn-Zn ferrites at high frequency by substituting In^{3+} and Al^{3+} ions *Ind. J. Pure & Appl. Phy*. **2008**, Vol-46, pp. 43. URL : http://hdl.handle.net/123456789/513 ISSN : 0019-5596

[9] Kadam, S.L.; Kanamadi, C. M.; Patankar, K. K.; Chougule, B. K. Dielectric behaviour and magneto electric effect in $Ni_{0.5}Co_{0.5}Fe_2O_4$ + Ba0. 8Pb0. $2TiO_3$ *ME composites Materials letters*, **2003**, Vol.59, pp. 215-219 DOI : 10.1016/S0254-0584(02)00352-8

[10] Kadam, S. L.; Patankar, K. K; Mathe, V. L.; Kothale, M. B.; Kale, R. B.; Chougule, B. K. Electrical properties and magnetoelectric effect in $Ni_{0.75}Co_{0.25}Fe_2O_4$+$Ba_{0.8}Pb_{0.2}TiO_3$ composites *Materials Chemistry and Physics*, **2003,** Vol. 78, Issue 3, 28 February pp. 684-690 https://doi.org/10.1016/S0254-0584(02)00352-8

[11] Mahajan R. P.; Patankar, K. K.; Burange, N. M.; Chaudhari, S. C.; Ghatage, A. K.; Patil, S. A.; Dielectric properties and electrical conduction of nickel ferrite-barium titanate composites *Indian J Pure & Appl Phys.* **AUGUST 2000,** VOL 38. pp. 615-620

[12] Mathe, V. L.; Patankar, K, K.; Patil, R. N.; Lokhande, C. D. Synthesis and dielectric properties of Bi_{1-} xNd_xFeO_3 perovskites *Journal of Magnetism and Magnetic Materials* **April 2004,** Volume 270, Issue 3, pp.380-388 https://doi.org/10.1016/j.jmmm.2003.09.004

[13] Hedaooa, P.S.; Badwaika*, D.S.; Suryawanshi, S. M.; Rewatkar, K.G. Structural and Magnetic Studies of Zn Doped Nickel Nanoferrites Synthesize by Sol-gel Auto Combustion *Method Materials Today: Proceedings* **2019**, Volume 15, Part 3, pp. 416-423 https://doi.org/10.1016/j.matpr.2019.04.102

[14] Kabbur, S. M.; Ghodake, U.R.; Nadargi, D.Y.; Kambale, R.C.; Suryavanshi, S.S. Effect of Dy3+ substitution on structural and magnetic properties of nanocrystalline Ni-Cu-Zn ferrites, *J. Magn. Magn. Mater*., **2018** vol. 451, pp. 665-675 https://doi.org/10.1016/j.jmmm.2017.12.006

[15] Leal, E. et.al Structural, textural, morphological, magnetic and electromagnetic study of Cu-doped NiZn ferrite synthesized by pilot-scale combustion for RAM application *Arabian Journal of Chemistry* **November 2020**, Volume 13, Issue 11, , pp.8100-8118 https://doi.org/10.1016/j.arabjc.2020.09.041

[16] Deepty, M. et.al. XRD, EDX, FTIR and ESR spectroscopic studies of co-precipitated Mn–substituted Zn–ferrite nanoparticles *Ceramics International* **15 April 2019,** Vol. 45, Issue 6, pp. 8037-8044 https://doi.org/10.1016/j.ceramint.2019.01.029

[17] Butter worth and Co. Ltd; Magnetic Materials and Their Applications, **1974**, Elsevier, London, C. Heck (Ed), https://doi.org/10.1016/C2013-0-01016-X

[18] Smit J.; Wijn H. P. J. Ferrites, John Wiley, **1959,** New York, ISBN-10 : 5882162025 ISBN-13 : 978-5882162022, pp.144-150

[19] Dimri, M. C.; Verma, A; Kashyap, S. C.; Dube, D. C.; Thakur, O. P.; Prakash, C. Structural, dielectric and magnetic properties of NiCuZn ferrite grown by citrate precursor method *Mater.Sci.Engin*. *B* **2006,** Vol. 133, pp.42-48. https://doi.org/10.1016/j.mseb.2006.04.043

[20] Rana, M. U.; Abbas T. The effect of Zn substitution on microstructure and magnetic properties of $Cu_{1-x}Zn_xFe_2O_4$ ferrite *Journal of Magnetism and Magnetic Materials* **April 2002**, Vol. 246, Issues 1–2, , pp. 110-114 https://doi.org/10.1016/S0304-8853(02)00037-9

[21] Singh, A. K.; Goel, T. C.; Mendiratta, R. G. Dielectric properties of Mn-substituted Ni–Zn ferrites *J. Appl. Phys.* **2002** , 91, pp.6626-6629 DOI: 10.1063/1.1470256

[22] Koops, C. G. On the Dispersion of Resistivity and Dielectric Constant of Some Semiconductors at Audio frequencies, *Phys. Rev*. **1951**, 83, 121 https://doi.org/10.1103/PhysRev.83.121

[23] Almessiere, M. A.; Slimani, Y. et.al. Microstructure, dielectric and microwave features of [Ni0.4Cu0.2Zn0.4](Fe2−xTbx)O4 ($x \leq 0.1$) nanospinel ferrites *Journal of Materials Research and Technology* **September–October 2020,** Volume 9, Issue 5, pp.10608-10623 https://doi.org/10.1016/j.jmrt.2020.07.094

[24] M.A. Almessiere, B. Unal, Y. Slimani, A.D. Korkmaz, A. Baykal, I. Ercan , Electrical properties of La^{3+} and Y^{3+} ions substituted Ni0.3Cu0.3Zn0.4Fe2O4 nanospinel ferrites Results Phys. **2019,** 15, pp. 102755 https://doi.org/10.1016/j.rinp.2019.102755

[25] Kolekar, C.B.; Kamble, P.N.; Kulkarni, S. G.; Vaingankar, A. S.; Effect of Gd3+ substitution on dielectric behaviour of copper-cadmium ferrites *J. Mater. Sci.* **1995,** 30, pp. 5784- 5488 https://doi.org/10.1007/BF00356721.

[26] Shaikh, M.; Bellad, S.S.; Chougule, B.K. Temperature and frequency-dependent dielectric properties of Zn substituted Li–Mg ferrites *Journal of Magnetism and Magnetic Materials* **May 1999,** Volume 195, Issue 2, pp. 384-390 https://doi.org/10.1016/S0304-8853(99)00138-9

[27] Berchamans, L.J.; Selvan, R. K.; Kumar, P.N.S.; Augustins, C.O.; Structural and electrical properties of $Ni_{1-x}Mg_xFe_2O_4$ synthesized by citrate gel process *Journal of Magnetism and Magnetic Materials* **August 2004**, Vol. 279, Iss.1, pp. 103-110 https://doi.org/10.1016/j.jmmm.2004.01.073

[28] Rathore, D.; Kurchania, R.; & Pandey, R. K. Influence of particle size and temperature on the dielectric properties of $CoFe_2O_4$ nanoparticles. *Int. J Miner Metall Mater.* **2014,** 21**,** pp. 408–414 https://doi.org/10.1007/s12613-014-0923-8

[29] Reddy, M. B.; and Reddy, P. V. Low-frequency dielectric behaviour of mixed Li-Ti ferrites *Journal of Physics D: Applied Physics* **1991,** Vol. 24, No. 6 pp. 975-981 https://doi.org/10.1088/0022-3727/24/6/025

[30] Shrotri, J. J.; Kulkarni S. D.; Deshpande C. E.; Mitra A.; Sainkar S. R.; Kumar, P. S. A.; Date, S. K. Effect of Cu Substitution on the Magnetic and Electrical Properties of Ni-Zn Ferrite Synthesized by Soft Chemical, *Materials Chemistry and Physics* **April 1999,** Vol. 59, No. 1, pp 1-5 doi:10.1016/S0254-0584(99)00019-X